DOI: 10.26599/FSHW.2024.9250107

Contents lists available at SciOpen

Food Science and Human Wellness

journal homepage: https://www.sciopen.com/journal/2097-0765

Effect of ellagitannin metabolites ellagic acid and urolithins A-D on the non-enzymatic glycation of human serum albumin and inhibiting mechanisms

Lu Zhang[1], Chun-yan Peng[1], Wen-na Zhou[1], Feiyan Lu[1], Linju Xu[1],Qinghui Wen[1], Xing Xie[1,*], Zong-cai Tu*[1,2]

[1] *National R&D center of Freshwater Fish Processing, College of Life Science, Jiangxi Normal University, Nanchang, Jiangxi 330022, China;*

[2] *State Key Laboratory of Food Science and Resources, Nanchang University, Nanchang, Jiangxi 330047, China*

ABSTRACT: Effect of ellagitannins gut microbiota metabolites ellagic acid (EA) and urolithin A-urolithin D (UroA-UroD) on human serum albumin (HSA) glycation were firstly evaluated in this research. The inhibition mechanisms were investigated by methylglyoxal (MGO) trapping and radical scavenging ability assays, docking studies and Nano LC-Orbitrap-MS/MS technology. Results indicated that the inhibition of urolithins on HSA glycation was highly positive correlated with the number of phenolic hydroxy groups. Addition of UroD and EA could effectively enhance the content of free amino group, suppress dicarbonyl compounds and advanced glycation end-products (AGEs) formation, alleviated tryptophan and protein oxidation, inhibited HSA amyloid-like aggregation. They could also trap MGO and scavenge DPPH· and $ABTS^{\cdot+}$. Molecular docking indicated that EA and UroA-UroD interact with HSA mainly through hydrogen bound and hydrophobic interaction, among which two or three hydrogen bonds were formed. The number of glycation sites were reduced from 11 to 10, 10, 7, and 10, respectively, when 90 μmol/L of EA, UroA, UroC and UroD were added. However, weak inhibition was observed on UroA and UroB. These findings can provide scientific evidence for the application of ellagitannins-rich foods in alleviating diabetic complications.

Keywords: Ellagitannin metabolites; human serum albumin; non-enzymatic glycation.

1. Introduction

Glycation reaction, also known as non-enzymatic glycosylation, is a nucleophilic addition reaction between the carboxyl group of reducing sugar and the free amino group of protein or peptide. Lysine, arginine, and the N-terminal of protein/peptide is the main potential glycosylation site [1, 2]. The extent of protein glycation in health people is limited, but in these suffer from diabetes, prolonged hyperglycemia will strongly promote the glycation of hemoglobin and serum albumin [3, 4]. Among which, glycated hemoglobin (HbA1c) is the international king-standard for evaluating the blood glucose status in clinical practice, and can reflect the average blood glucose levels of diabetes within 2 − 3 months, as well as the risk of diabetic complications [5]. However, hemoglobin is an intracellular protein, glucose cannot react with hemoglobin before being transported into erythrocyte through glucose transporter 1. What's more, it

***Corresponding author**
Prof. Zong-cai Tu, E-mail: tuzc_mail@aliyun.com.
Dr. Xing Xie, E-mail: 13609092537@163.com

Received 5 May 2023
Received in revised from 22 August 2023
Accepted 7 October 2023

contains much less potential glycation sites (lysine and arginine residues) than serum protein [6]. It was reported that serum protein undergoes glycation before hemoglobin and is the main target of glycation [7].

Human serum albumin (HSA) is the most abundant plasma protein and responsible for multiple biological activities, like binding and transporting endogenous and exogenous compounds (such as drugs, nutrients, etc.), regulating plasma pH and lipid metabolism, maintaining osmotic pressure, and anti-oxidation, etc. Due to the long half-life (14 − 20 days), free circulation in body, and massive free lysine and arginine residues (85 glycation sites), HSA is highly sensitive to post-translational modifications, especially for glycation modifications [8]. In diabetic patients, HSA is more susceptible to undergo non-enzymatic glycosylation as compared with other proteins, and is the major glycated target, accounting for approximately 80% of the total glycated proteins in the blood [9]. Currently, glycated HSA has been used as a supplementary indicator of HbA1c or real-time blood glucose monitoring, which can indicate the average blood glucose levels of diabetic patients within 21 days [10]. Glycation can not only change the two- and three-dimensional structure of HSA, resulting to the alteration in antioxidant activity and molecular transporting function [11, 12], but also can form many advanced glycation end-products (AGEs), active oxygen and active carbon free radical, causing irreversible damage to bioactive macromolecules, organs and tissues [10]. It was reported that glycation of HSA would promote thrombosis formation, inhibit glucose uptake of cells, evoke inflammatory responses, and increase the risk of cardiovascular complications, etc [9, 13]. In addition, the accumulation of AGEs in the body could accelerate the progress of diabetic complications, such as cardiovascular disease, kidney damage, Alzheimer's disease and retinal damage [14]. Hence, inhibiting HSA glycation is of great importance for relieving diabetic complications and other related sub-health status.

Ellagitannins (ETs) is a class of hydrolyzable tannins founding naturally in many fruits and nuts, such as pomegranate, strawberries, walnuts, black teas, almonds, and oaks, et al., and was reported to show a large number of biological activities, but it cannot be absorbed directly in the gastrointestinal tract upon ingestion [15]. In the stomach and gut digestion stage, ETs undergo hydrolysis and produce hexahydroxydiphenoyl (HHDP) group, which is then spontaneously converted into ellagic acid (EA). Some of the EA can be absorbed in gastrointestinal tract, the unabsorbed EA are subsequently metabolized by gut microbiota to form a lot of 3,8-dihydroxy-6H-dibenzopyran-6-one type derivatives, also named as urolithin intermediates, such as urolithin A (UroA), urolithin B (UroB), urolithin D (UroD), and urolithin C (UroC) (**Fig.1**) [16]. Urolithins (Uros) are much better absorbed and exhibit higher bio-availability than the original ETs and EA, and were also evidenced to be responsible for the health effects of ET-rich foods consumption [17]. Up to date, plenty of bio-activities have been found on EA and Uros, such as extending lifespan, preventing cardiovascular diseases, alleviating inflammatory reaction, anti-oxidant, anti-diabetes, anti-cancer and anti-obesit [18, 19]. Liu et al. [20] indicated that UroA, UroB, and EA could suppressed fructose-induced bovine serum albumin glycation by scavenging

reactive carbonyl species, and EA showed the strongest activity. Our previous research found UroA could inhibit the formation of AGEs in HSA-fructose system by trapping methylglyoxal, promoting the exposure of chromophores to more hydrophobic micro-environment, and forming UroA-HSA complexes [21]. However, the structure-activity relationship of ET metabolites inhibiting HSA glycation, as well as its effect on the formation of glycation products and further inhibition mechanism are still unclear.

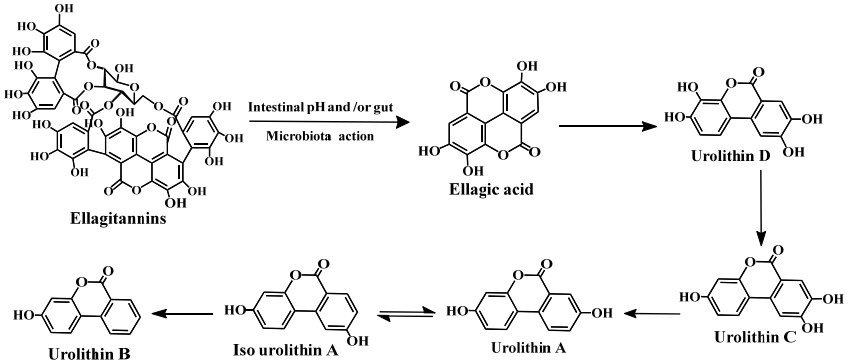

Fig.1 A simple schematic view for the gut microbiota metabolism of ellagitannin and ellagic acid in gastrointestinal tract.

In this research, the inhibition of EA, UroA, UroB, UroC, and UroD on HSA glycation were evaluated by determining the formation of fructosamine, dicarbonyl compounds, fluorescent AGEs, and oxidation products. Influences on the fibrotic situation and molecular weight of native and glycated HSA were studied with fluorescence spectroscopy and sodium dodecyl sulfate polyacrylamide gel electropheresis (SDS-PAGE). The inhibition mechanisms were analyzed by methylglyoxal (MGO) trapping ability, free radical scavenging capability assays, and Nano liquid chromatography system coupled to Orbitrap tandem mass spectrometry (Nano LC-Orbitrap-MS/MS) technique. This study can provide a theoretical basis for EA and Uros as non-enzymatic glycosylation inhibitors to prevent diabetic complications and related sub-health state.

2. Materials and methods

2.1 Reagents and chemicals

O-phenylenediamine (O-PDA), acetone aldehyde, 5-methylquinoxaline (5-MQ), trypsin, HSA (Code: A1653), 2,2′-azino-bis-3-ethylbenzthiazoline-6-sulphonic acid (ABTS), dithiothreitol (DTT), iodoacetamide (IAA), and 1,1-diphenyl-2-picrylhydrazyl (DPPH) were purchased from Sigma-Aldrich (Louis, USA). EA, UroA, UroB, UroC, and UroD were from Shanghai YuanYe Biotechnology Co., Ltd. (Shanghai, China). Glucose, aminoguanidine hydrochloride (AG), nitro-blue tetrazolium (NBT), methanol, formic acid, trichloroacetic acid, sodium dodecyl sulfate (SDS), 2-nitrobenzoic acid (DTNB), thioflavin T (ThT), and acetonitrile (ACN) were purchased from Shanghai Aladdin Technology Co., Ltd (Shanghai, China). All other chemicals and reagents were analytical grade and purchased from Solarbio Biological Technology Co., Ltd. (Beijing, China).

2.2 HSA-glucose model assay

The HSA-glucose glycation model was performed according to previous report[21]. Glucose (0.5 M) and HSA (20 mg/mL) solution were prepared with 0.1 M, pH 7.4 phosphate buffered saline (PBS). EA and UroA-UroD were dissolved in dimethyl sulfoxide (DMSO). Then, 1.0 mL of HSA, 1.0 mL of glucose and 200 μL of 1.0 mmol/L EA, UroA-UroD or AG were mixed and incubated at 37 ºC for 4 weeks. The control group and blank group without inhibitors or glucose were prepared in parallel. After the incubation, all sample were kept at 4 ºC for further analysis.

2.3 Determination of free amino group, fructosamine, dicarbonyl compound, and fluorescent AGEs

The free amino group contents of all samples were estimated with fluorogenic OPA method [22]. 2 mL OPA reagent were mixed with 100 μL of samples in tube, and incubated for 5 min at room temperature. Subsequently, the absorbance of complexes was measured at 340 nm. Lysine (0 − 1250 μg/mL) was used as standards to calculate the content of amino groups. $y = 474.87x - 139.19$, $R^2 = 0.9981$. The results were expressed as lysine equivalent (μg/mL protein).

Determination of fructosamine content was conducted based on the NBT method [23]. Briefly, 20 μL of glycated mixtures prepared in section 2.2 and 180 μL of 1.0 mmol/L NBT solution (pH=10.8, 0.1 M carbonated buffer solution) were reacted at 37 ℃ for 2.0 h. The absorbance at 530 nm was measured by microplate reader (Biotek, Vermont, USA), and used to reflect the relative content of fructosamine.

The dicarbonyl compounds was evaluated according to the description of Liu et al [20]. The glycated samples (40.0 μL) were mixed with Girard-T reagent (100 μL, 0.5 M) and sodium formate (1.7 mL, 0.5 M, pH 2.9) in sequence, and allowed to react at 37 ℃ for 1.0 h. Then, absorbance at 290 nm was measured by microplate reader (Biotek, Vermont, USA).

The inhibition on fluorescent AGEs formation was measured by the method previously reported [21]. The percentage inhibition was calculated with the maximum fluorescence intensity.

$$\text{Inhibition}(\%) = \frac{(FI_c - FI_b) - (FI_s - FI_{nb})}{FI_c - FI_b} \times 100\% \qquad (1)$$

where FI_c, FI_b, FI_s and FI_{nb} are the fluorescence intensity of control group, blank group, experimental group, and sample blank group, respectively.

2.4 Oxidation products

2.4.1 Determination of free tryptophan

The free tryptophan was determined by fluorescence spectroscopy [24]. All sample solutions were 10-fold diluted and used for fluorescence intensity evaluation at an excitation and emission wavelength of 280 and 350 nm, respectively. The slit width and PMT voltage were set at 2.5 nm and 700 V, respectively. The scanning rate is set as 1200 nm/min. The fluorescence intensity could indicate the relative tryptophan content.

2.4.2 Determination of free thiol groups

Change in free thiol groups (-SH) on HSA was determined using 5,5′-dithiobis, DTNB method [1]. Glycated sample (50 μL) was mixed with 50 μL of 3.0 mmol/L DTNB solution, 150 μL of 100 mmol/L ethylene diamine tetraacetic acid (EDTA) in 96-well microplate. After 20 min of reaction at 37 ℃, absorbance at 412 nm was monitored using a microplate reader. Blank group was prepared with samples replaced by double distilled water, the concentration of free thiol group was calculated based on the standard curve plotted with L-cysteine and expressed as microgram L-cys per milliliter of sample solution (μg L-cys/mL).

2.5 Effect of EA and UroA-UroD on the structure of glycated HSA

2.5.1 Thioflavin T fluorescence

The fibrotic state of protein was investigated by the ThT method [25]. The glycated samples or native HSA and ThT solution (10 μg/mL) were mixed in equal volume, following by 40 min of incubation at 25 °C. Thereafter, fluorescence intensity at an excitation wavelength of 450 nm and emission wavelength of 490 nm was measured by a F-7000 fluorescence spectrophotometer (Hitachi, Japan).

2.5.2 SDS-PAGE

The SDS-PAGE experiment was performed according to previous method with slight modifications [26]. All samples were pre-treated with buffer and then loaded (10 μL, 250 μg/mL) into each well of 10% SDS-PAGE gel. Then, electrophoresis was performed at 80 volts for 3 h at room temperature. Protein was stained with Coomassie Brilliant Blue (CBBR-250) for 30 min followed by destaining with water overnight.

2.6 Molecular docking

The 3D structure of HSA (PDB ID: 1AO6) was acquired from protein data bank (www.rcsb.org/structure/1AO6). The 3D structure of EA and UroA-UroD were achieved from PubChem website (https://pubchem.ncbi.nlm.nih.gov/) and their PubChem CID numbers were EA (5281855), UroA (5488186), UroB (5380406), UroC (60198001) and UroD (5482042), respectively [21]. Before docking analysis, the structure of HSA was optimized by removing duplicate sequences, non-catalytic water molecules, and adding a polar hydrogen and charge. The molecular docking was analyzed with Discovery Studio 2020 software. The size of grid was set at 60 × 60 × 60 Å with a grid spacing of 15.2798 Å. The binding site was set at domain III with the center co-ordinates of (13.25, 29.20, 21.98) along the X, Y, and Z axis, which was accorded with other studies [21]. The docking calculations were run for 100 times by Genetic Algorithm, the output was sorted by Lamarckian GA module, the conformations with the minimum energy of EA and UroA-UroD with HSA were selected as docking results. The binding energy was calculated by the following formula: Binding Energy = Complex Energy - Ligand Energy - Receptor Energy.

2.7 Nano LC-Orbitrap-MS/MS analysis

2.7.1 Sample preparation

The digestion and hydrolyzation of samples were carried out according to our previous method [27]. Freeze-dried glycated HSA were dissolved in 200 μL of SDT buffer (4% SDS, 100 mmol/L Tris-HCl, 1 mmol/L DTT, pH 7.6) and boiled for 5 min. Then 50 μL of boiled samples were mixed with 200 μL of urea buffer (8.0 M Urea, 150 mmol/L Tris-HCl, pH 8.0) in 10 kDa ultrafiltration centrifuge tube (Sartorius, Germany), and centrifuged at 14,000 g for 15 min. After centrifugation one more time with urea buffer, 100 μL of IAA (50 mmol/L IAA in UA buffer) was added and incubated at 25 ºC for 30 min in darkness. The tubes were centrifuged at 14, 000 g for 10 min, the proteins remained in the upper part were then successively washed with 100 μL of urea buffer for three times. Finally, 40 μL of trypsin buffer (2 μg of trypsin in 40 μL of 25 mmol/L NH_4HCO_3) was added to hydrolyze HSA at 37 ℃ for 16 h. The proteolytic peptides were collected by centrifugation at 14, 000 g for 10 min and used for peptide mapping.

2.7.2 Nano LC-Orbitrap-MS/MS analysis

An Easy-nLC1000 system couple to a tandem mass spectrometer was used for peptides and glycation site identification. Two microliters of proteolytic peptides was injected into an Acclaim PepMap 100 RP-C18 loading column (2 μm, 100 μm × 2 cm, Thermo Scientific, Waltham, MA, U.S.A.) coupled to an Acclaim PepMap RSLC RP-C18 analytical column (2 μm, 75 μm × 15 cm, Thermo Scientific, Waltham, MA, U.S.A.). The column was eluted with 0.1% aqueous formic acid (solvent A) and acetonitrile containing 0.1% formic acid (solvent B) at a flow rate of 300 nL/min, and equilibrated with 4% B for 7 min before injection. The elution of gradient was: (0 – 6) min, 4% B; (6 – 50) min, 4% (B – 25)% B; (50 – 58) min, 25% B – 40% B; (58 – 61) min, 40% B – 85% B; (61 – 66) min, 85% B. The mass spectrometry (MS) and tandem mass spectrometry (MS/MS) data were collected using an Orbitrap fusion mass spectrometer (Thermo Scientific, Waltham, MA, U.S.A.). The operating parameters were as follows: positive ion model; MS scanning range, m/z 350 − 1800; MS resolution, 60000; MS/MS fragmentation mode, high-energy C-trap dissociation (HCD) and electron transfer dissociation (ETD); MS/MS resolution, 15 000; automatic gain control (AGC) target, 4 × 105; maximum injection time (IT), 50 ms; dynamic exclusion, 60 s; and normalized collision energy, 30 eV.

2.8 MGO trapping ability

The trapping capacity of EA and UroA-UroD on methylglyoxal (MGO) was determined by high performance liquid chromatography (HPLC) [28]. Briefly, 250 μL of 5.0 mmol/L MGO and 250 μL of 200 μmol/L EA or UroA-UroD solutions were added in brown bottles with caps. They were then incubated in a constant temperature shaking incubator at 40 r/min, 37 ℃ for 24 h, followed by the addition of 5.0 μL acetic acid to terminate the reaction. Then, 50 μL of 5.0 mmol/L o-PDA and 50 μL of internal standard 5-MQ (5.0 mmol/L) were added and allowed to incubate at 25 ℃ for 30 min. They were finally filtered with 0.22 μm nylon membrane and subjected to HPLC analysis. The HPLC analytical parameters were: injection volume of 30 μL; ZORBAX SB-C18 column (4.6 mm × 250 mm, 5 μm, Japan); Solvent A and B consisted of 0.1% formic acid-water and acetonitrile, respectively. The gradient elution program were: (0 − 5) min,

5% B; (5.5 − 20.0) min, 35% − 40% B; (20.5 − 25.5) min, 95% B; (26.0 − 30.0) min, 5% B. The trapping ability was calculated based on the peak area.

2.9 Radical scavenging ability assays

To compare the radical scavenging ability of EA and UroA-UroD, DPPH· and $ABTS^{\cdot+}$ scavenging ability assays were conducted following reported methods [23]. Fifty microliters EA or UroA-UroD (1.0 mmol/L) solution were reacted with 150 μL of freshly prepared DPPH· (0.15 mmol/L) or $ABTS^{\cdot+}$ (absorbance of 0.70 ± 0.20 at 734 nm) solution in 96-well microplate. After certain times of incubation in darkness at room temperature, absorbance (As) at 517 and 734 nm was measured individually for DPPH· and $ABTS^{\cdot+}$ scavenging ability. Aminoguanidine was set as positive control, the percentage scavenging ability was calculated as following:

$$\text{Scavenging ability } (\%) = \frac{(A_c - A_b) - (A_s - A_b)}{(A_c - A_b)} \times 100\% \qquad (2)$$

where, A_c was the absorbance of control group with samples replaced by distilled water; A_b was the absorbance of blank group with radical solution replaced by ethanol.

2.10 Statistical analysis

All experiments were performed in triplicate, the values were presented as mean value ± standard deviation (SD). Statistical analysis of data was evaluated by SPSS software (SPSS 22.0, IBM, Armonk, NY, USA) via one-way analysis of variance (ANOVA), a value of $P < 0.05$ was considered to show significant difference.

3. Results and discussions

3.1 Contents of glycation HSA products

3.1.1 Effect of EA and UroA-UroD on the formation of fructosamin

Fructosamine is the early glycation products, as one of the indexes for clinical evaluation of diabetes, its level is usually positively correlated with blood glucose concentration [29]. Effect of EA and UroA-UroD on the content of fructosamine was shown in **Fig.2A**. The A_{530} values were significantly enhanced in UroC group and increased by 26.17% compared with the glycated HSA without inhibitor (G-HSA) ($P < 0.05$), followed by the EA and UroD group, and no significant difference was observed between these two groups ($P > 0.05$). Whereas, the addition of UroA (0.667) and UroB (0.693) had no obvious effect on the absorbance at 530 nm as comparison to that of G-HSA (0.703) ($P > 0.05$). Above results indicated that EA, UroB, UroC, and UroD could promote the accumulation of fructosamine in HSA-glucose glycation system, UroC gave the strongest effect.

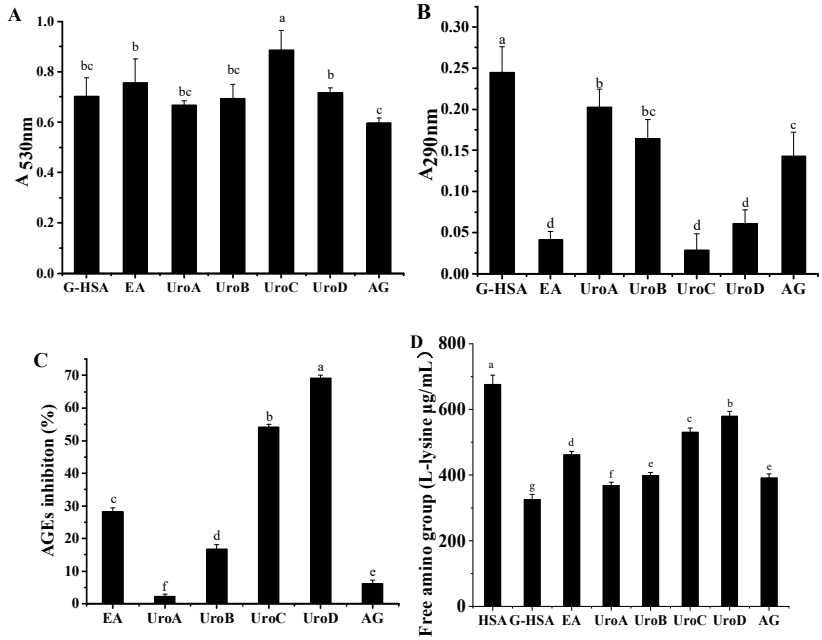

Fig.2 In the HSA-glucose model, effect of EA, UroA-UroD and AG on the formation of fructosamine (A), α-dicarbonyl compounds (B), AGEs (C) and free amino group (D). Different letters indicate statistically significant differences ($P < 0.05$). The concentrations of EA, UroA-UroD and AG in HSA-glucose model were 90.90 μmol/L.

3.1.2 Suppression of EA and UroA-UroD on the formation of dicarbonyl compounds

Dicarbonyl compounds are typical middle glycation products, they are highly reactive and can attack quickly with the free amino group of protein to form fluorescent AGEs. Therefore, inhibiting dicarbonyl compounds accumulation has been an important aspect of natural small molecular to suppress protein glycation [20, 28]. Effect of EA and UroA-UroD on the production of dicarbonyl compounds was displayed in **Fig.2B**, the absorbance at 290 nm (A_{290} value) reflects the relative content. It's clear that the G-HSA group gave the highest A_{290} value of 0.245, the addition of EA, UroA-UroD and AG could significantly reduce the A_{290} value ($P < 0.05$), especially for EA, UroC, and UroD, the average value was reduced to 0.041, 0.029, and 0.061, respectively ($P < 0.05$). Therefore, it could be concluded that EA and UroA-UroD could suppress the dicarbonyl compounds formation in HSA-glucose glycation system, EA, UroC, and UroD exhibited much higher effect than UroA and UroB. Liu et al. [20] also found that EA showed higher capturing ability on typical dicarbonyl compounds methylglyoxal than UroA and UroB.

3.1.3 Inhibition of EA and UroA-UroD on the formation of fluorescent AGEs

Fluorescent AGEs are typical end-products of protein glycation, so, the inhibitory ability of EA and UroA-UroD on the late stage of HSA glycosylation were evaluated by measuring the inhibition on fluorescent AGEs formation. According to **Fig.2C**, the best fluorescent AGEs inhibitory rate was detected on UroD, followed by UroC. The percentage inhibition at the concentration of 90 μmol/L was 69.31% and 54.21%, respectively. While, negligible inhibitory rate was observed on UroA (2.33%) and positive control AG (6.14%), which differed from the results found in previous reports, it could be due to the low concentration used in this research. The EA (28.15%) and UroB (16.80%) showed certain inhibition, but the ability was much weaker than that of UroC and UroD. The results were highly negatively correlated ($R^2 = -0.73$) to the

dicarbonyl compounds content, indicating the importance of trapping or suppressing dicarbonyl compounds on alleviating fluorescent AGEs formation. Liu et al. [20] and Peng et al. [21] individually proved that scavenging dicarbonyl compounds was one of the mechanism of EA and UroA suppressing fluorescent AGEs formation.

3.1.4 Influence of EA and UroA-UroD on free amino group

The free amino groups of proteins like ε-NH2 groups of lysine will interact with the carbonyl groups of sugars during glycation reaction, and resulted to the decrease of free amino groups, which was an important indicator to reflect the effect of samples on HSA glycation [30]. As shown in **Fig. 2D**, the content of free amino groups in natural HSA was 675.80 μg/mL, which was reduced to 325.47 μg/mL after glycation, while it was returned to (367.85 − 579.05) μg/mL with the addition of EA, UroA-UroD and AG. The results indicated that EA, UroA-UroD and AG could hinder the free amino groups of HSA to bind with sugars, delayed the process of glycation, UroC and UroD showed the best effects. Similar findings were observed in the studies of Arfin et al. [30], who found that addition of isoferulic acid significantly reduced the content of free amino groups in HSA-fructose system.

3.2 Analysis of oxidation products

3.2.1 Contents of tryptophan

The tryptophan residues can be oxidized by free radical produced during glycation process, resulting in reduced fluorescence intensity at an excitation and emission wavelength of 280 and 350 nm, respectively [24]. The oxidation products of tryptophan were divided into tryptophan-Amadori products and (1R,3S)-1-(D-gluco-1,2,3,4,5-pentahydroxypentyl)-1,2,3,4-tetrahydro-β-carboline-3-carboxylic acid (Ph-TH*β*C), which can promote the progress of protein glycation [31]. As displayed in **Fig.3A**, the fluorescence intensity of tryptophan residues on natural and glycated HSA was 148.33 and 59.64, respectively, suggesting that 59.79% of tryptophan residues in HSA were oxidized after glycation. Addition of EA and UroD alleviated the fluorescence intensity weaken of G-HSA, the fluorescence intensity was enhanced by 45.00% and 54.81%, respectively, as compared with G-HSA. Addition of UroC and AG showed insignificant influence on the fluorescence intensity of G-HSA ($P > 0.05$), unexpectedly, UroA and UroB reduced the fluorescence intensity obviously. Therefore, it can be seen that EA and UroD could effectively inhibited tryptophan oxidation, and the inhibitory ability of Uros was highly correlated to the number of phenolic hydroxyl groups on the dibenzopyran-6-one ring.

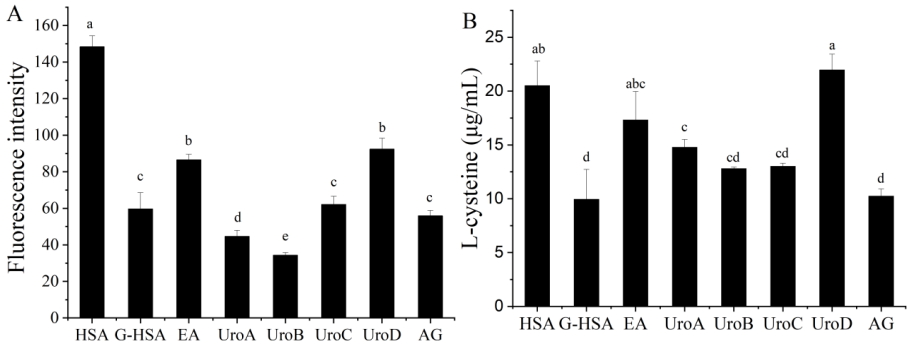

Fig.3 Effect of EA, UroA-UroD and AG on tryptophan residues (A) and free thiol group content (B) in the HSA-glucose model. Different letters indicate statistically significant differences ($P < 0.05$). The concentrations of EA, UroA-UroD and AG in HSA-glucose model were 90.90 μmol/L.

3.2.2 Contents of free thiol groups

Levels of free thiol groups is the indicator of protein redox status, and provides a evidence for protein conformational change [32, 33]. Effect of EA, UroA-UroD, and AG on free thiol level were evaluated and the results were given in **Fig.3B**, the amount of free thiol groups in native HSA was 20.50 μg L-cys /mL, it decreased to 9.95 μg L-cys /mL as a result of glycation. However, the content of free thiol was returned to almost native HSA levels upon the addition of EA and UroD ($P > 0.05$), the amount was enhanced to 17.31 and 21.96, respectively. UroA could also enhance the content of free thiol to 14.77 μg CyE/mL, but the ability was much lower than that of UroD. However, insignificant difference was observed on the HSA glycated in the presence of UroB, UroC, and AG ($P > 0.05$). These findings demonstrated that EA, UroA, and UroD could protect HSA from oxidation during non-enzymatic glycosylation, UroD exhibited the strongest activity. Qais et al. [1] also reported that glyburide inhibited the non-enzymatic glycosylation of HSA by mitigating the degradation of the free thiol groups degradation.

3.3 Change on the structure of glycated HSA

3.3.1 Effect of EA and UroA-UroD on the aggregation of G-HSA

The fluorescent AGEs formed during glycation can induce protein cross-linking to form amyloid-like aggregation, leading to alteration of protein structure and function. Currently, attenuating the amyloid aggregation of proteins has been a potential target for evaluating the ability of compounds or extracts against protein glycation [34]. ThT is a biomarker that can bind to the β-sheet structure present in amyloid fibrils, and then displays a strong fluorescence in the emission wavelength of 480-490 nm upon excited at 440 nm [25]. Therefore, ThT was used to evaluate the fibrillar state of native and glycated HSA, the results were presented in **Fig.4A**. Native HSA presented the minimal fluorescence intensity (370.91), which was increased to 588.53 upon glycated with glucose, suggesting obvious fibrillar formation and HSA aggregation. The presence of EA, UroB, and UroD reduced the ThT fluorescence of G-HSA significantly, the intensity decreased by 28.5%, 21.5%, and 22.8%, respectively, and exhibited insignificant difference ($P > 0.05$). Addition of UroA, UroC, and AG could also diminish the ThT fluorescence of G-HSA ($P > 0.05$), but the ability was weaker than that of EA, UroB, and UroD. Above results implied that EA and UroA-UroD could prevent the amyloid aggregation of HSA induced by glucose glycation, and EA, UroB, and UroD demonstrated stronger effect.

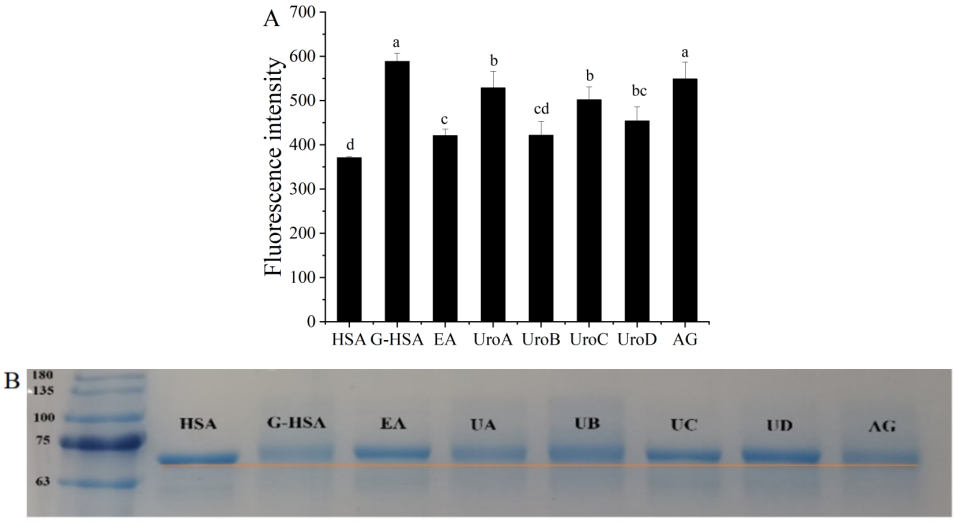

Fig.4 Influence of EA, UroA-UroD and AG on the fibrillar state (A) and molecular weight of glycated and native HSA (B). Different letters indicate statistically significant differences ($P < 0.05$). The concentrations of EA, UroA-UroD and AG in HSA-glucose model were 90.90 μmol/L.

3.3.2 Effect of EA and UroA-UroD on the molecular weight of HSA

The native HSA, glycated HSA, and G-HSA with EA and UroA-UroD were applied to SDS-PAGE analysis to elucidate the influence of glycation and EA and UroA-UroD on the molecular weight of HSA. As shown in **Fig.4B**, native HSA gave an obvious dark protein band at about 68 kDa, which is consistent with the molecular weight of HSA (66 kDa), but the glycated HSA has no obvious dark protein band at the same position of native HSA, the band exhibited slight upshift, indicating the increment of molecular weight, in addition, the color of the band was much lighter. The colour of protein band in the presence of EA, UroC, and UroD were darker compared with that of G-HSA, this could be that addition of EA, UroC, and UroD alleviated the increase of HSA molecular weight induced by glycation, and relieved the dispersion phenomenon of band, especially for UroD, the position and color of G-HSA with UroD was close to that of G-HSA. Similar results were obtained in previous reports, Abdullah et al. [26] found that pyridoxamine could effectively reduce the electrophoretic mobility of glycated HSA medicated by glucose. Min et al. [35] indicated that the molecular weight enhancement and protein dispersion of glycated HSA were alleviated by epigallocatechin gallate.

3.4 Molecule docking analysis

Molecular docking is the common methods to investigate the interaction mechanism between small molecule compounds and protein [33, 36]. Molecular docking simulation can better understand the structural changes between food proteins and small molecules at the molecular level [37, 38]. Many studies show that HSA had two primary binding sites, subdomain IIA and subdomain IIIA, and the small molecule compounds were more likely to bind in subdomain IIIA [21]. The binding energy for the interaction of EA and UroA-UroD with HSA were − 44.97, − 16.27, − 20.43, − 7.73 and − 38.73 kcal mol^{-1}, respectively, suggesting that the binding of EA and HSA was the most stable, followed by UroD. As shown in Fig.5, EA UroA, UroB, UroC, and UroD formed three, two, two, three and three hydrogen bonds with the amino acid

residues in subdomain IIIA of HSA, respectively. In addition, Pi-cation and Pi-alkyl interactions were also participated in the binding of EA and UroA-UorD with HSA, which enhanced the affinity. With HSA-EA complex as example, three hydrogen bonds were formed between the hydroxyl or aldehyde groups of EA and the amino acid residues of Arg410, Tyr411 and Leu430, and EA also interacted with the amino acid residues of Leu407, Leu453, Val433, and Arg485 by Pi-alkyl interactions. The results indicated that hydrophobic interactions and hydrogen bonds were the major driving force to bind EA or UroA-UroD with HSA, which possibly hindered the glycation sites of HSA, resulting the inhibition on the progress of HSA [1].

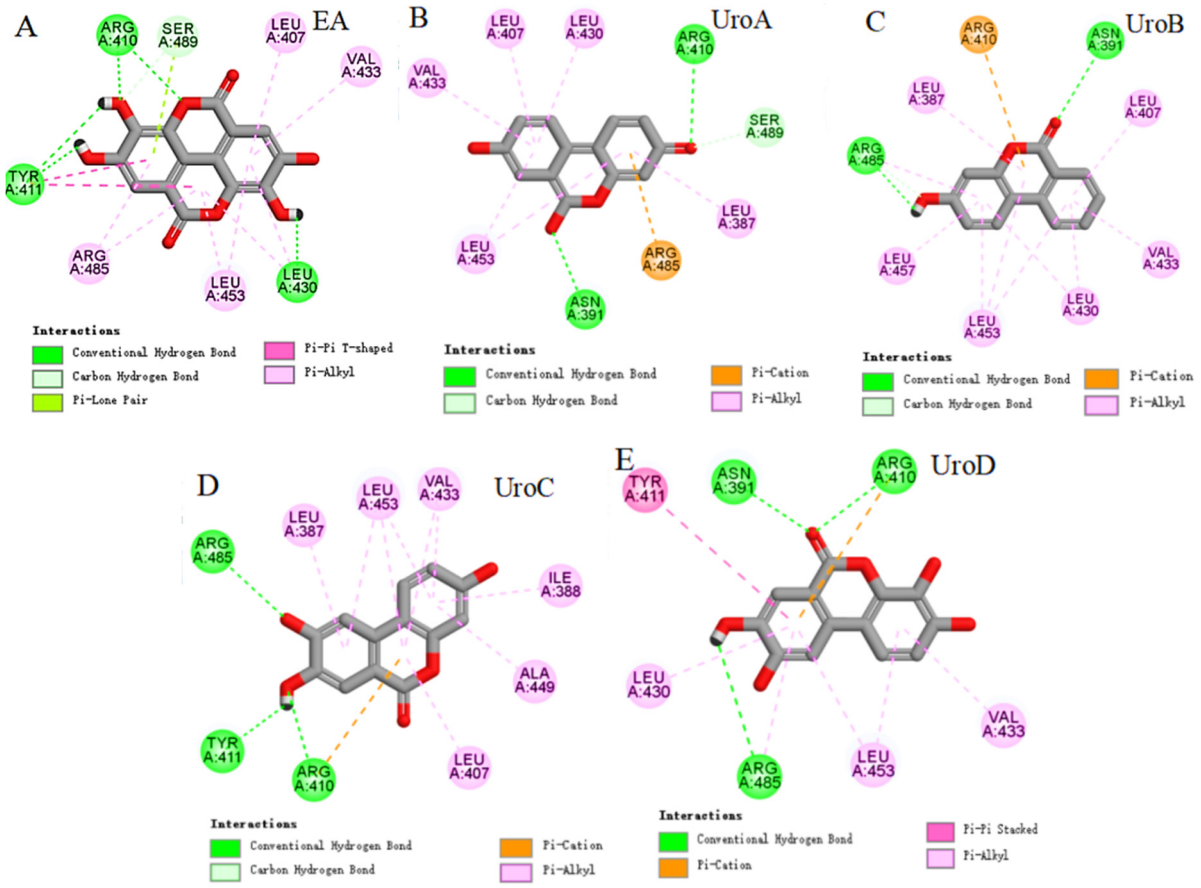

Fig.5 The 2-dimensional plot of EA and UroA-UroD interact with HSA by Discovery Studio 2020.

To better understand the mechanism of EA and UroA-UroD attenuating HSA glycation, the glycated peptides and glycation sites were identified by Nano LC-Orbitrap-MS/MS after ultrafiltration and hydrolyzation of G-HSA with and without inhibitors. The amino acid sequence of proteolytic peptide was identified by matching the parent ions (m/z) and fragmentation ions (b-series and y-series ions) with that recorded in database Uniport Homo sapiens (https://prospector.ucsf.edu/ prospector/mshome.htm). The glycated peptides were mapped according to the mass shift before and after glycation. Theoretically, when a molecular of glucose was attached, the corresponding m/z will display a mass shift of 162.0528, 81.0264, 54.0176, 40.5132, and 32.4106 for these in charge of 1, 2, 3, 4, and 5, respectively. The glycation locations were further identified by matching the b-series and y-series ions with that recorded in database Uniport Homo sapiens. In case of a peptide contains m amino acid residues, the mass shift between c(n) and c(n-1), z(m-n+1) and z(m-n) will be 162+128 or 162+156, respectively, when one molecule of glucose was attached to the Lys

or Arg residues at the site location n [27]. For example, the peak with m/z at 387.4538^{4+} was identified as peptide ^{290}LKECCEKPLLEK^{310} as shown in **Fig.6A**, its singly and doubly glycated form will exhibit a mass shift of 40.5132 and 81.0261, respectively, resulting to the corresponding occurrence of peaks at 427.9668^{4+} and 468.4799^{4+}. Interesting, these two glycated peaks were both detected on the MS spectra, implying two molecules of glucose were attached. The m/z of peptide ^{589}ET(CAM)CFAEEGKK^{598} at unglycated and glycated pattern was 400.1842^{3+} and 454.2017^{3+}, respectively, indicating the mass shift of 54.0171 (shown in **Fig.6B**). Thus, it could be concluded that peptide 589 − 598 was glycated by one molecule of glucose. In terms of glycation sites identification, the m/z peak of C8 and C9 was 941.3629 and 1231.5087, respectively, indicating the mass shift of 290.1458. Therefore, the attachment of one glucose was at Lys597 other than Lys598. In light of this theory, glycated peptide 585 − 598 (ADDKETCFAEEGKK, shown in **Fig.6C**) possessed three potential glycation sites (K588, K597, and K598), the mass shift between ions C4 (m/z, 609.2679) and C3 (m/z, 319.1232), C13 (m/z 1822.7571) and C12 (m/z, 1532.6018) were both at 290, suggesting the molecular weight of a glucosyl and a Lys588/Lys597 residue. Thus, Lys588 and Lys597 were proposed as the glycated position.

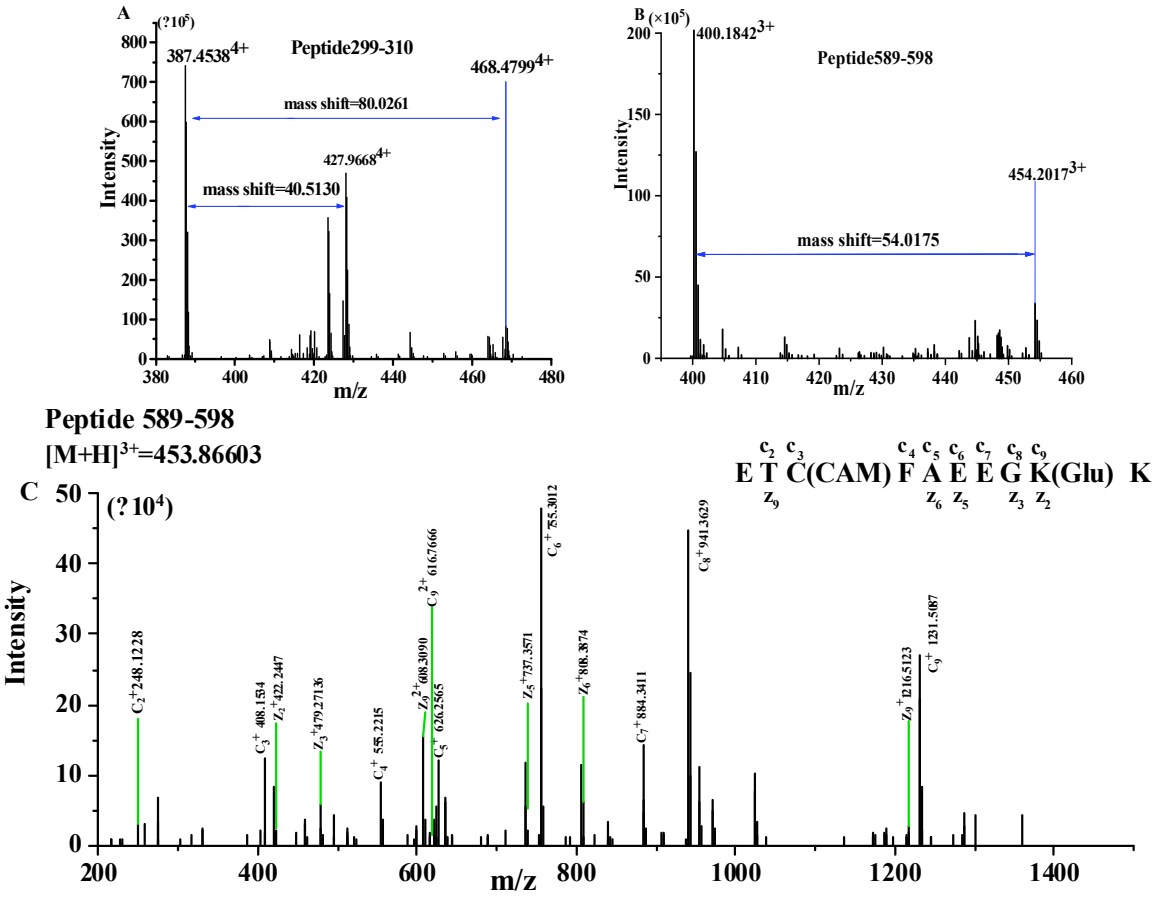

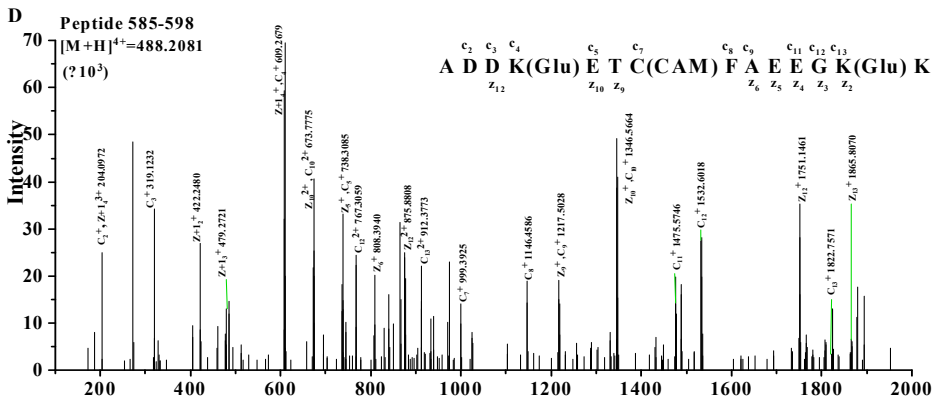

Fig.6 The MS spectra of glycated peptide 290-310 with m/z of 468.4799^{4+} (A) and glycated peptide 589-598 with m/z of 454.2017^{3+} (B). The HCD MS/MS spectra of glycated peptide 589-598 (ETCFAEEGKK) (C) and peptide 585-598 (ADDKETCFAEEGKK) (D).

The detailed glycation peptides and glycation sites identified in G-HSA with and without inhibitors were listed in **Table 1**. Eleven sites Lys130, Lys186, Lys300, Lys305, Lys341, Lys499, Lys549, Lys558, Lys588, Lys597, and Lys598 were detected in G-HSA. After the addition of EA, UroA, UroB, UroC, and UroD, the number of glycated sites were 10, 10, 11, 7, and 10, respectively. Sites Lys186, Lys305, Lys341, Lys499, Lys597, and Lys598 disappeared in the G-HSA with UroC, but new sites Lys214 and Lys569 appeared, which further proved that UroC alleviated the number of glycated sites. UroA could completely inhibit sites Lys300, Lys341, and Lys558. In addition, glycation sites Lys36, Lys161, and Lys438 appeared in G-HSA in the presence of EA, but sites Lys186, Lys305, Lys499, and Lys598 disappeared. After the addition of UroD, one glycation site was reduced, only Lys36, Lys88, Lys130, Lys160, Lys205, Lys257, Lys305, Lys341, Lys549, and Lys588 were identified. The addition of UroB did not change the number of glycation sties, but the glycated sites was different. Therefore, it can be seen that EA and UroA-UroD could alter the glycation sites of HSA, and UroC decreased the sites number greatly. Qais et al. [1] proposed that glyburide might decreased the available sites of glycation on HSA by masking of free amino groups of HSA. Peng et al. [21] also evidenced that UroA could reduce the glycation reactivity of some sites by altering conformation structure of HSA and changing the micro-environment nearby potential glycation sites.

3.6 Trapping of EA and UroA-UroD on MGO

MGO is a typical dicarbonyl compound, it can attack the free amino group of protein to form fluorescent AGEs, trapping MGO can effectively reduce MGO-mediated protein glycation and fluorescent AGEs formation [28]. Therefore, the MGO trapping ability of EA and UroA-UroD were evaluated to further analyze the mechanism of EA and UroA-UroD inhibiting HSA glycation. As shown in **Fig.7A**, the MGO trapping ability of EA, UroA, UroB, UroC, and UroD at 90 μmol/L was 72.92%, 7.80%, 69.15%, 46.37%, and 89.72%, respectively. UroD gave the strongest trapping ability, followed by EA and UroB ($P > 0.05$), the ability was all much stronger than that of positive control AG (49.99%). UroC exhibited insignificant MGO trapping ability as compared with AG ($P > 0.05$). Unexpectedly, UroA showed a much weaker trapping ability at the concentration of 90 μmol/L, which is similar with the results reported by Liu et al., [20] who found that UroA

reduced 10.1% of MGO at a concentration of 500 μmol/L. These results indicated that EA and UroA-UroD could trap MGO and hinder HSA glycosylation. Peng et al. [21] also indicated that UroA could inhibit fluorescent AGEs formation in HSA-glucose system by trapping MGO.

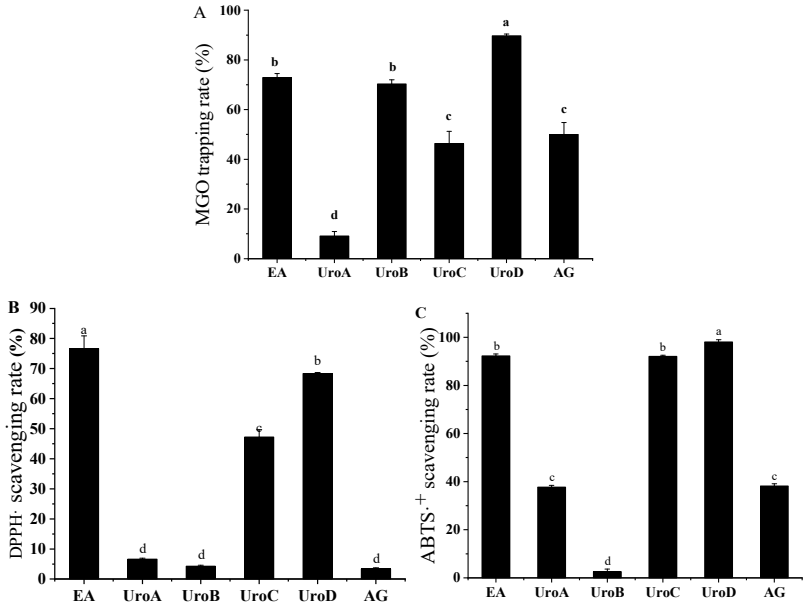

Fig.7 The MGO trapping ability (A) and DPPH· (B) and ABTS·$^{+}$ scavenging activity (C) of EA, UroA-UroD and AG. Different letters indicate statistically significant differences ($P < 0.05$). The concentrations of EA, UroA-UroD and AG in HSA-glucose model were 90.90 μmol/L.

3.7 Antioxidant capacity

In this research, the DPPH· and ABTS·$^{+}$ scavenging ability assays were conducted to compare the radical scavenging ability of EA and UroA-UroD. Non-enzymatic glycosylation of proteins, glucose auto-oxidation and carbonyl stress can all induce free radicals production, which in turn accelerate fluorescent AGEs formation and the development of diabetes and diabetic complications [39, 40]. Anti-oxidant compounds such as flavonoids, phenolic acid, polysaccharides, and vitamins have been demonstrated to reduce protein glycosylation *in vivo* and *in vivro* [41]. Thus, radical scavenging ability could be one of the mechanism for compounds against protein glycosylation. The scavenging ability of EA and UroA-UroD on DPPH· and ABTS·$^{+}$ were given in **Fig.7B** and **Fig.7C**. EA, UroC, and UroD exhibited good DPPH· scavenging ability at the sample concentration of 250 μmol/L, and followed the order of EA (76.68%) > UroD (68.34%) > UroC (47.24%). While UroA, UroB, and AG all showed negligible scavenging ability on DPPH· ($P > 0.05$). In terms of ABTS·$^{+}$, UroD had the strongest scavenging ability, followed by EA and UroC ($P > 0.05$), while UroB exhibited the weakest ability, the scavenging ability was close to zero at 250 μmol/L. These are consistent with the results found by Bialonska et al., [42] who found that UroC and UroD possessed much higher antioxidant ability than UroA and EA through HL-60 cells assay, no antioxidant ability was detected on UroB, and proposed that the antioxidant potential of urolithins depends on the number of hydroxyl substitution.

3.8 Correlation analysis

Currently, trapping reactive carbonyl and reactive oxygen species, altering protein conformation, restraining protein oxidation and aggregation, forming stable complexes, and reducing the glycation reactivity of glycation sites were the revealed mechanism of natural compounds against HSA glycation [1, 25, 43]. This research indicated that EA, UroC, and UroD greatly restrained the formation of dicarbonyl compounds and fluorescent AGEs in HSA-glucose system, EA and UroD exhibited stronger inhibition on the oxidation of tryptophan and HSA than UroA-UroC. In addition, better alleviation on the molecular increment of HSA induced by glycation was observed on UroC and UroD than UroA and UroB. EA, UroA, UroC, and UroD obviously inhibited the fibrillar of HSA and altered the sites glycated, and UroC decreased the number of glycated sites mostly. What's more, UroC, UroD, and EA presented excellent and better MGO trapping ability, DPPH· and $ABTS^{+}$· scavenging activity than UroA and UroB. UroA, UroB, UroC, and UroD is urolithin carrying two (3'-OH and 8'-OH), one (3'-OH), three (3'-OH, 4'-OH, and 8'-OH), and four (3'-OH, 4'-OH, 8'-OH, and 9'-OH) hydroxyl groups, respectively (**Fig.1**), EA also possesses four hydroxy groups. The stronger bio-abilities detected on UroC, UroD and EA than UroB and UroA could be attributed to the greater number of hydroxyl groups. Correlation analysis revealed high correlation coefficients (R^2, shown in **Table S1**) between the number of hydroxyl groups and the dicarbonyl compounds content ($R^2 = -0.85$), fluorescent AGEs formation inhibition ($R^2 = -0.91$), tryptophan oxidation (free tryptophan content, $R^2 = -0.96$), contents of free amino group (lysine content, $R^2 = 0.93$), DPPH· ($R^2 = 0.97$) and $ABTS^{+}$· scavenging activity ($R^2 = 0.95$). Dicarbonyl compounds and fluorescent AGEs are typical middle and advanced glycation products, suppressing the formation are usually used as the key indicators to evaluate the anti-glycation ability of compounds or natural extracts, high negative R^2 also suggested the importance of hydroxyl group in the anti-glycation ability of urolithins.

In addition, significantly correlation between radical scavenging activities and dicarbonyl compounds content, fluorescent AGEs formation inhibition, free tryptophan and thiol content, with the R^2 ranged from 0.93 to 0.75, suggesting the important role of antioxidant ability on inhibiting harmful glycation products formation and protein oxidation. This could be that dicarbonyl compounds are highly reactive carbonyl species and middle products, it can attack quickly the free amino group of protein to form fluorescent AGEs and lead to protein oxidation. Compounds with higher radical scavenging usually shows stronger dicarbonyl compounds capturing ability, therefore exhibited better mitigation on protein glycation. Previous researches indicated that cinnamic acid restrained HSA glycation by scavenging reactive carbonyl species and dampening protein oxidation due to the antioxidant capacity [25], the inhibition of glucose auto-oxidation by antioxidants reduced the covalent linking of glucose to serum albumin [44], administration of vitamin E could effectively reduce protein glycosylation in diabetic patients [45]. Nadeem et al. [46] found that addition of antioxidants diethylenetriamine pentaacetic acid and dithiothreitol could improve the level of fructosamine during glycation, while reactive oxygen radical exhibited a negative impact.

What's more, the dicarbonyl compounds content showed good negatively correlated (**Table S1**) with fluorescent AGEs percentage inhibition rate ($R^2 = -0.73$), tryptophan oxidation ($R^2 = -0.80$), protein

oxidation ($R^2 = -0.63$) and fibrillar ($R^2 = -0.65$), indicating the importance of trapping or suppressing dicarbonyl compounds on the alleviation of EA and UroA-UroD on HSA glycation. Currently, trapping dicarbonyl compounds was reported to be the one of the major mechanism of natural compounds against protein glycation, such as quercetin [47], hesperetin-Cu [48], cichoric acid [49] (ACN) were purchased , rosmarinic acid [25], punicalagin and ellagic acid [20] and vitexin [28] etc.

4. Conclusion

In summary, the inhibition of urolithins on HSA glycation was highly depended on the number of phenolic hydroxy groups, stronger anti-glycation was observed on EA, UroC, and UroD as compared with UroA and UroB. UroD presented the strongest inhibition activity on fluorescent AGEs formation with the inhibition rate of 69.31 % at 90 μmol/L, followed by UroC. Obviously, suppression on dicarbonyl compounds formation was also observed on EA, UroC, and UroD ($P > 0.05$). Meanwhile, EA and UroD could effectively increase the level of tryptophan residues, free amino and free thiol groups, prevent amyloid aggregation of HSA induced by glycation, trap MGO, and scavenge DPPH· and $ABTS^{\cdot+}$. Molecular docking analysis indicated EA and UroA-UroD formed complex with HSA through hydrogen bonds and hydrophobic interaction, 2-3 hydrogen bonds Pi-alkyl and Pi-cation interactions were detected between EA or UroA-UroD and the amino acid residues of HSA, which might hinder the glycation sites and ultimately inhibited the glycation procession. In addition, addition of EA, UroC, and UroD might alter the availablity of glycation sites on HSA, the number of glycated sites was reduced by 1, 4 and 1, respectively. Overall, trapping MGO, scavenging free radicals, suppressing protein oxidation and cross-linking, and altering the glycation activity of potential sites all contributed to inhibition of EA, UroC, and UroD on HSA glycation. This study could provide theoretical support for the application of ellagitannins-rich foods, or EA and UroC-UroD as glycation inhibitors to alleviate harmful glycation products formation *in vivo*.

Declaration of Interest

The authors declare that they have no known competing financial interests or personal relationships that could have appeared to influence the work reported in this paper.

Acknowledgments

This research was supported by the Natural Science Foundation of Jiangxi Province (20212BAB205017, 20192ACB21011) and National Science and Technology Award Reserve Cultivation Program Project of Jiangxi (20212AEI91001).

References

[1] F.A. Qais, T. Sarwar, I. Ahmad, et al., Glyburide inhibits non-enzymatic glycation of HSA: an approach for the management of AGEs associated diabetic complications, Int. J. Biol. Macromol 169 (2021) 143-152. https://doi.org/10.1016/j.ijbiomac.2020.12.096.

[2] N.S. Bangar, A. Gvalani, S. Ahmad, et al., Understanding the role of glycation in the pathology of various non-communicable diseases along with novel therapeutic strategies, Glycobiology 32 (2022) 1068-1088. https://doi.org/10.1093/glycob/ cwac060.

[3] X. Liu, N. Wu, A. Al-Mureish, A review on research progress in the application of glycosylated hemoglobin and glycated albumin in the screening and monitoring of gestational diabetes, Int. J. Gen. Med 14 (2021) 1155-1165. https://doi.org/10.2147/ IJGM.S296316.

[4] S. Ahmad, M.Y. Khan, Z. Rafi, et al., Oxidation, glycation and glycoxidation-the vicious cycle and lung cancer, Semin Cancer Biol 49 (2018) 29-36. https://doi.org/ 10.1016/j.semcancer.2017.10.005.

[5] J. Nicholas, J. Charlton, A. Dregan, et al., Recent HbA1c values and mortality risk in type 2 diabetes. population-based case-control study, PLoS One 8 (2013) e68008. https://doi.org/10.1371/journal.pone.0068008.

[6] R.L. Garlick, J.S. Mazer, The principal site of nonenzymatic glycosylation of human serum albumin in vivo, J. Bio. Chem 258 (1983) 6142-6146. https://doi.org/10.1016/ S0021-9258(18)32384-6.

[7] S. Bhat, M.G. Jagadeeshaprasad, V. Venkatasubramani, et al., Abundance matters: Role of albumin in diabetes, a proteomics perspective, Expert. Rev. Proteomic 14 (2017) 677-689. https://doi.org/10.1080/14789450.2017.1352473.

[8] M. Zendjabil, Glycated albumin, Clin. Chim. Acta 502 (2020) 240-244. https://doi. org/10.1016/j.cca.2019.11.007.

[9] H.Y. Qiu, N.N. Hou, J.F. Shi, et al., Comprehensive overview of human serum albumin glycation in diabetes mellitus, World J Diabetes 12 (2021) 1057-1069. https:// doi.org/10.4239/wjd.v12.i7.1057.

[10] P.A.C. Freitas, L.R. Ehlert, J.L. Camargo, Glycated albumin: A potential biomarker in diabetes, Arch. Endocrin Metab 61 (2017) 296-304. https://doi.org/10.1590/2359-3997000000272.

[11] K. Neelofar, Z. Arif, K. Alam, et al., Hyperglycemia induced structural and functional changes in human serum albumin of diabetic patients: A physico-chemical study, Mol. Biosyst 12 (2016) 2481-2499. https://doi.org/10.1039/ c6mb00324a.

[12] H. Qiu, L. Jin, J. Chen, et al., Comprehensive glycomic analysis reveals that human serum albumin glycation specifically affects the pharmacokinetics and efficacy of different anticoagulant drugs in diabetes, Diabetes 69 (2020) 760-770. https://doi. org/10.2337/db19-0738.

[13] S. Arques, P. Ambrosi, Human serum albumin in the clinical syndrome of heart failure, J. Card. Fail 17 (2011) 451-458. https://doi.org/10.1016/j.cardfail.2011. 02.010.

[14] W. Rungratanawanich, Y. Qu, X. Wang, et al., Advanced glycation end products (AGEs) and other adducts in aging-related diseases and alcohol-mediated tissue injury, Exp. Mole. Med 53 (2021) 168-188. https://doi.org/10.1038/s12276-021-00561-7.

[15] S.A. Al-Harbi, A.O. Abdulrahman, M.A. Zamzami, et al., Urolithins: the gut based polyphenol metabolites of ellagitannins in cancer prevention, a review, Front Nutr 8 (2021). https://doi.org/10.3389/fnut.2021.647582.

[16] A. Peiroten, D. Bravo, J.M. Landete, Bacterial metabolism as responsible of beneficial effects of phytoestrogens on human health, Crit. Rev. Food. Sci. Nutr 60 (2020) 1922-1937. https://doi.org/10.1080/10408398.2019.1622505.

[17] F.A. Tomas-Barberan, A. Gonzalez-Sarrias, R. Garcia-Villalba, et al., Urolithins, the rescue of "old" metabolites to understand a "new" concept: Metabotypes as a nexus among phenolic metabolism, microbiota dysbiosis, and host health status, Mol. Nutr. Food Res. 61 (2017) 1500901. https://doi.org/10.1002/mnfr.201500901.

[18] S.H. Hasheminezhad, M. Boozari, M. Iranshahi, et al., A mechanistic insight into the biological activities of urolithins as gut microbial metabolites of ellagitannins, Phytother Res 36 (2022) 112-146. https://doi.org/10.1002/ptr.7290.

[19] D. D'Amico, P.A. Andreux, P. Valdes, et al., Impact of the natural compound urolithin A on health, disease, and aging, Trends Mol. Med 27 (2021) 687-699. https://doi.org/ 10.1016/j.molmed.2021.04.009.

[20] W. Liu, H. Ma, L. Frost, et al., Pomegranate phenolics inhibit formation of advanced glycation endproducts by scavenging reactive carbonyl species, Food Funct 5 (2014) 2996-3004. https://doi.org/10.1039/c4fo00538d.

[21] C.Y. Peng, H.D. Zhu, L. Zhang, et al., Urolithin A alleviates advanced glycation end-product formation by altering protein structures, trapping methylglyoxal and forming complexes, Food Funct 12 (2021) 11849-11861. https://doi.org/10.1039 /d1fo02631c.

[22] L. Zhang, Y. Lu, Y.H. Ye, et al., Insights into the mechanism of quercetin against BSA-fructose glycation by spectroscopy and high-resolution mass spectrometry: effect on physicochemical properties, J. Agr. Food. Chem 67 (2019) 236-246. https://doi. org/10.1021/acs.jafc.8b06075.

[23] X. Wu, G. Zhang, M. Hu, et al., Molecular characteristics of gallocatechin gallate affecting protein glycation, Food Hydrocolloids 105 (2020) 105782. https://doi.org/ 10.1016/j.foodhyd.2020.105782.

[24] M.A.J. Al Jaseem, K.M. Abdullah, F. Abul Qais, et al., Mechanistic insight into glycation inhibition of human serum albumin by vitamin B9: Multispectroscopic and molecular docking approach, Int. J. Biol. Macromol 181 (2021) 426-434. https://doi.org/10.1016/j.ijbiomac.2021.03.153.

[25] A. Shamsi, A. Ahmed, M.S. Khan, et al., Rosmarinic acid restrains protein glycation and aggregation in human serum albumin: Multi spectroscopic and microscopic insight - possible therapeutics targeting diseases, Int. J. Biol. Macromol 161 (2020) 187-193. https://doi.org/10.1016/j. ijbiomac.2020.06.048.

[26] K.M. Abdullah, F.A. Qais, I. Ahmad, et al., Study of pyridoxamine against glycation and reactive oxygen species production in human serum albumin as model protein: An in vitro & ex vivo approach, Int. J. Biol. Macromol 120 (2018) 1734-1743. https://doi.org/10.1016/j.ijbiomac.2018.09.176.

[27] L. Jia, L. Zhang, Y.H. Ye, et al., Effect and mechanism of elaeagnus angustifolia flower and its major flavonoid tiliroside on inhibiting non-enzymatic glycosylation, J. Agr. Food. Chem 67 (2019) 13960-13968. https://doi.org/10.1021/acs.jafc.9b06712.

[28] M. Ni, X. Song, J. Pan, et al., Vitexin inhibits protein glycation through structural protection, methylglyoxal trapping, and alteration of glycation site, J. Agr. Food. Chem 69 (2021) 2462-2476. https://doi.org/10.1021/acs.jafc.0c08052.

[29] M.S. Khan, M.S. Alokail, A.M.H. Alenad, et al., Binding studies of caffeic and p-coumaric acid with alpha-amylase: Multispectroscopic and computational approaches deciphering the effect on advanced glycation end products (AGEs), Molecules 27 (2022). https://doi.org/10.3390/molecules27133992.

[30] S. Arfin, G.A. Siddiqui, A. Naeem, et al., Inhibition of advanced glycation end products by isoferulic acid and its free radical scavenging capacity: An in vitro and molecular docking study, Int. J. Biol. Macromol 118 (2018) 1479-1487. https://doi.org/10.1016/j.ijbiomac.2018.06.182.

[31] M. Friedman, J.L. Cuq, Chemistry, analysis, nutritional value, and toxicology of tryptophan in food. A review, J. Agric. Food. Chem 36 (1988) 1079-1093. https://doi.org/10.1021/jf00083a042.

[32] A. Shamsi, M. Shahwan, F.M. Husain, et al., Characterization of methylglyoxal induced advanced glycation end products and aggregates of human transferrin: Biophysical and microscopic insight, Int. J. Biol. Macromol 138 (2019) 718-724. https://doi.org/10.1016/j.ijbiomac.2019.07.140.

[33] M.S. Khan, M.T. Rehman, M.A. Ismael, et al., Bioflavonoid (Hesperidin) restrains protein oxidation and advanced glycation end product formation by targeting AGEs and glycolytic enzymes, Cell. Biochem. Biophys 79 (2021) 833-844. https://doi.org/10.1 007/s12013-021-00997-8.

[34] I. Sirangelo, C. Iannuzzi, Understanding the role of protein glycation in the amyloid aggregation process, Int. J. Mol. Sci 22 (2021) 6609-6629. https://doi.org/10.339 0/ijms22126609.

[35] M. Li, A.E. Hagerman, Effect of (-)-epigallocatechin-3-gallate on glucose-induced human serum albumin glycation, Free Radical Res 49 (2015) 946-53. https://doi.org/1 0.3109/10715762.2015.1016429.

[36] X. Hu, Z. Zeng, J. Zhang, et al., Molecular dynamics simulation of the interaction of food proteins with small molecules, Food Chem 405 (2023) 134824. https:// doi.org/10.1016/j.foodchem.2022.134824.

[37] W. Wu, X. Hu, Z. Zeng, et al., Characterization of the binding properties of sorafenib to c-MYC G-quadruplexes: Evidence for screening potential ligands, J. Phys. Chem. B 1 (2023) 1520-6106. https://10.1021/acs.jpcb.2c06488874J.

[38] M. Li, D. Zhou, D. Wu, et al., Comparative analysis of the interaction between alpha-lactalbumin and two edible azo colorants equipped with different sulfonyl group numbers, Food Chem 416 (2023) 135826. https://doi.org/10.1016/j.foodchem.2023.135826.

[39] A.D. SM, O. Rebolledo, Lipoprotein glycation and glycoxidation: their importance in diabetes mellitus, Medicina 60 (2000) 645-656.

[40] L. Zhang, Q. M. Zhou, L. Xu, et al., Extraction optimization and identification of four advanced glycation-end products inhibitors from lotus leaves and interaction mechanism analysis, Food Chem 414 (2023) 135712. https://doi.org/10.1016/j.foodchem.2023.135712.

[41] A. Ceriello, A. Quatraro, D. Giugliano, New insights on non-enzymatic glycosylation may lead to therapeutic approaches for the prevention of diabetic complications, Diabetic Med 9 (1992) 297-299. https://doi.org/10.1111/j.1464-5491.1992.tb01783.x.

[42] D. Bialonska, S.G. Kasimsetty, S.I. Khan, et al., Urolithins, intestinal microbial metabolites of Pomegranate ellagitannins, exhibit potent antioxidant activity in a cell-based assay, J. Agr. Food. Chem 57 (2009) 10181-10186. https://doi.org/10.1021/jf9025794.

[43] F.A. Qais, M.M. Alam, I. Naseem, et al., Understanding the mechanism of non-enzymatic glycation inhibition by cinnamic acid: an in vitro interaction and molecular modelling study, RSC Advances 6 (2016) 65322-65337. https://doi.org/ 10.1039/c6ra12321j.

[44] J.V. Hunt, R.T. Dean, S.P. Wolff, Hydroxyl radical production and autoxidative glycosylation. Glucose autoxidation as the cause of protein damage in the experimental glycation model of diabetes mellitus and ageing, Biochemical J 256 (1988) 205-212. https://doi.org/10.1042/bj2560205.

[45] A. Ceriello, D. Giugliano, A. Quatraro, et al., Vitamin E reduction of protein glycosylation in diabetes: new prospect for prevention of diabetic complications?, Diabetes Care 14 (1991) 68-72, https://doi.org/10.2337/diacare.14.1.68.

[46] N.A. Ansari, Moinuddin, A.R. Mir, et al., Role of early glycation amadori products of lysine-rich proteins in the production of autoantibodies in diabetes type 2 patients, Cell Biochem Biophys 70 (2014) 857-865, https://doi.org/10.1007/s12013-014-9991-7.

[47] X. Li, T. Zheng, S. Sang, et al., Quercetin inhibits advanced glycation end product formation by trapping methylglyoxal and glyoxal, J. Agr. Food. Chem 62 (2014) 12152-8. https://doi.org/10.1021/jf504132x.

[48] P. Xi, H. Xing, L. Kai, et al., Exploring inhibitory effect and mechanism of hesperetin-Cu (II) complex against protein glycation, Food Chem 416 (2023) 135801. https://doi.org/ 10.1016/j.foodchem.2023.135801.

[49] Y. P. Zhang, C. Y. Zhang, M. F. Wang, et al., Effect of macromolecular crowding on the inhibition of non-enzymatic glycation of bovine serum albumin by cichoric acid, Food Biosci 53 (2023) 102801. https://doi.org/10.1016/j.fbio.2023.10280.